COVER SHEET

Characterization of iodine particles with Volatilization-Humidification Tandem Differential Mobility Analyser (VH-TDMA), Raman and SEM techniques

Z.D. Ristovski[1], C. Fletcher[1], B. D'anna[2], G.R. Johnson[1] and J. T. Bostrom[3]

[1]{International Laboratory for Air Quality and Health, School of Physical and Chemical Sciences, Queensland University of Technology, GPO Box 2434, Brisbane, QLD 4001, Australia}

[2]{Spectroscopic Group, Department of Chemistry, University of Oslo, P.O.Box 1033 Blindern, 0315 Oslo, Norway}

[3]{Analytical EM Facility, School of Physical & Chemical Sciences; Queensland University of Technology, Australia}

Correspondence to: Z.D. Ristovski (z.ristovski@qut.edu.au)

Abstract

Particles formed upon photo-oxidation of CH_2I_2 and particles of I_2O_5 and HIO_3 have been studied using a Volatilisation and Humidification Tandem Differential Mobility Analyser (VH-TDMA) system. Volatilization and hygroscopic behaviour have been investigated as function of temperature (from 25 to 400°C), humidity (RH from 80 to 98%), initial aerosol sizes (from 27 to 100 nm mobility diameter) and in nitrogen or air as the sheath gasses. The volatility behaviour of particles formed upon photo-oxidation of CH_2I_2 is more similar to that of HIO_3 particles in a filtered sheath air than in nitrogen, with the particle shrinkage occurring at 190°C and accompanied by hygroscopic growth. Despite its high solubility, HIO_3 was found not to be hygroscopic at room temperature with no significant growth displayed until the thermodenuder temperature reached 200°C or above when the particles have transformed into I_2O_5. Diiodopentaoxide (I_2O_5) particles exhibit relatively low hygroscopic growth factors of 1.2-2 in the humidity range investigated. Scanning Electron Microscopy (SEM) of particles formed upon photo-oxidation of CH_2I_2 shows that their primary elemental components were

iodine and oxygen in a stoichiometric ratio of approximately 1:2 with 10% error. Both Raman spectra and SEM show poor crystallinity for all the aerosols produced.

1 Introduction

Aerosols are known to have direct and indirect effects on Earth's in-coming and out-going solar radiation, resulting in a radiative forcing which is negative (cooling effect) (IPCC, 2001). In addition, the aerosols influence the albedo of the Earth by acting as cloud condensation nuclei (CCN) and thereby affecting the formation of clouds (Twomey et al., 1984). The most likely mechanisms for new particle formation in the troposphere appear to be binary nucleation of sulphuric acid and water vapour, and ternary nucleation of sulphuric acid ammonia and water vapour. (Kulmala et al., 2002; Kulmala et al., 2000; Napari et al., 2002; Van Dingenen and Raes, 1993; Wyslouzil et al., 1991). However, intense nucleation bursts have been observed in the marine/coastal boundary layer, and appear to be associated with the presence of gaseous iodine species (O'Dowd et al., 1998; O'Dowd et al., 2002a; O'Dowd et al., 2002b). Laboratory studies on the photo-oxidation of iodocarbons (CH_2I_2 and CF_3I) in presence of ozone demonstrate the possibility of generating nucleation-mode particles from condensable iodine vapours (CIVs) in the absence of sulphur species (Burkholder et al., 2003; Hoffmann et al., 2001; Jimenez et al., 2003; O'Dowd et al., 2002c). Measurements of molecular iodine in the marine boundary layer (MBL) (Saiz-Lopez and Plane, 2004) and laboratory studies on the photo-oxidation of macroalgae emissions *(Laminaria)* reveal the possibility that molecular iodine in the presence of ozone and light may also contribute to new particle formation (McFiggans et al., 2004). In both cases, photo-oxidation of diiodiomethane and molecular iodine, the particles formed show very similar composition. (McFiggans et al., 2004) Composition analysis performed by Aerodyne Aerosol Mass Spectrometry (AAMS) indicates the presence of iodine oxides, oxy-acids and water (Jimenez et al., 2003; McFiggans et al., 2004).

Hygroscopicity is a key parameter in the study of growth, visibility, cloud activation, reactivity and atmospheric lifetime of aerosols (Ansari and Pandis, 2000) but may also be used to differentiate between particle compositions, provided the component compounds/mixtures differ in hygroscopic growth. During the PARFORCE field campaign, the newly formed particles (modes 8-10 nm) showed low growth hygroscopic factors

(between 1.0 and 1.1) (Vakeva et al., 2002). Particles produced upon photo-oxidation of molecular iodine with O_3 showed growth factors between 1.0 (for 60 nm particles) to 1.2 (for 20 nm particles) at RH = 90% (McFiggans et al., 2004). The mobility diameter of particles formed upon photo-oxidation of CH_2I_2 in dry conditions (RH< 23 %) decreased when exposed to humid air, reaching a minimum growth factor of 0.66. In contrast particles produced in humid air (RH> 65%) showed a constant growth factor of ca. 1.0 when exposed to 90% RH. So far this intriguing behaviour has been explained in terms of fractal structure for particles produced in dry conditions (Jimenez et al., 2003).

The low growth factors and the particles density, 3.5 g/cm^3, seem to designate I_2O_4 as the most suitable candidate (Jimenez et al., 2003), however a definitive assignment to the particle composition has not been established. The volatilization-humidification tandem differential mobility analyser (VH-TDMA) (Johnson et al., 2005) provides a useful technique for the characterisation of physico-chemical properties of aerosols and in reducing the range of candidates for the composition of an unknown aerosol (Rader and McMurry, 1986). The instrument combines the possibility of differentiating on the basis of the particles' growth response to humidification (which depends on the chemical properties of the aerosol), and of investigating the aerosol's volatilisation characteristics.

The present work investigates: (I) the hygroscopic growth and volatility of diiodopentoxide (I_2O_5) and iodic acid (HIO_3) for which no measurements have been reported in the literature to date; (II) the volatilization and hygroscopic behaviour of particles formed upon photo-oxidation of diiodiomethane with ozone under controlled conditions. The above physico-chemical properties are reported as a function of temperature (ranging from 25 to 350°C), size (from 27 nm up to 140 nm), humidity (from 80 to 98 % RH) and carrier gas (ambient air or dry nitrogen); (III) Raman spectra of the aerosols; (IV) Scanning Electron Microscopy (SEM) analysis of the particles formed upon photo-oxidation of diiodiomethane with ozone. The results for the three systems have been critically compared.

2 Instrumentation

2.1 VH-TDMA

The volatility and hygroscopic tandem differential mobility analysis (VH-TDMA) system was used to characterize the physico-chemical properties of iodine aerosols. This system, shown schematically in Fig. 1 allows determination of the effect on an aerosol's size distribution of heating, and subsequently humidification. These physical properties, especially the response to humidity, provide direct information about how the aerosol would respond to different ambient conditions. It is also possible to make inferences about chemical components and composition from the extent of hygroscopic growth, the deliquescence point, the temperature at which volatile components evaporate, and the size of the aerosol after volatile components are removed.

The design of the VH-TDMA used in this study has been described in detail elsewhere (Johnson et al., 2005; Johnson et al., 2004a; Johnson et al., 2004b). Dry filtered aerosol is first passed through a differential mobility analyzer (DMA) to produce a size-classified aerosol fraction. This then passes through a heater where volatile components are removed through vaporization or decomposition to gaseous species.

A portion of the resulting heat-treated and charged aerosol is then examined for changes in particle diameter using a second DMA. The remaining portion of the volatilization-conditioned aerosol is examined in terms of its hygroscopic behavior using a humidification aerosol conditioner and a third DMA.

The VH-TDMA system was flow calibrated using a primary volume flow standard (Sensidyne Gilibrator-2 bubble flow meter) prior to commencement and flows were checked daily. Particle sizing accuracy was also checked using NIST traceable standard 102 nm polystyrene latex (PSL) spheres (Duke Scientific Corporation), injected downstream of the sheath air filter of the initial classifier stage after bypassing the saturator and allowing the humidifier column to dry. This method has the advantage of allowing the sizing accuracy of the second and third stages to be checked without changing the instrument plumbing configuration.

Humidity in the humidification column was tested throughout the experiment by examining the growth of dry NaCl aerosol in the VH-TDMA. The aerosol was produced by atomizing a NaCl solution and passing it through a silica gel diffusion dryer.

Few additions were made to the original design (Johnson et al., 2004b). First, in order to achieve relative humidity higher than 90%, a bypass line was added to DMA3. The limiting factor for the humidity was the mixing ratio between the dry air coming from the thermodenuder and the humid air coming from the saturator. Without the bypass line this ratio is equal to the ratio between the polydisperse inlet and sheath air inlet. With the addition of the bypass this ratio could be increased to 1:20 which enabled us to achieve relative humidities up to nearly 98%. Second, to be able to rapidly change the humidity in the humidifier, a bypass line was added to the saturator.

2.2 Aerosol Generation and Treatment

Aerosols were produced in two different ways: 1) by nebulising a water solution of the desired components and 2) by photochemical reaction of CH_2I_2 with O_3.

2.2.1 Nebulisation of a water solution

HIO_3 and NaCl aerosols were generated by a three jet Collision nebuliser (BGI Incorporated) from aqueous solutions prepared with ultra pure deionised water. The generated particles were first dried in a diffusion dryer of silica gel (RH ~ 5%), then sent to the first DMA.

Commercial I_2O_5 usually exists in its partially or fully hydrated form as $I_2O_5 \cdot HIO_3$ or HIO_3 respectively (Greenwood and Earnshaw, 1997); and HIO_3 can easily be formed after exposure of diiodopentoxide to water or humid air (Chase, 1996).

$$\frac{1}{2}I_2O_5 + \frac{1}{2}H_2O \longrightarrow HIO_3$$

The HIO_3 aerosol was therefore produced by nebulising a solution of dissolved commercial I_2O_5 and ultra pure water. The particles are expected to revert back to I_2O_5 upon dehydration in the thermodenuder at 180-200 °C (Chase, 1996).

$$3\,HIO_3 \xrightarrow{70°C} I_2O_5 \cdot HIO_3 + H_2O$$
$$2\,I_2O_5 \cdot HIO_3 \xrightarrow{200°C} 3\,I_2O_5 + H_2O$$

I_2O_4 oxide may be generated in several ways, through reaction of HIO_3 with concentrated H_2SO_4 (Bahl and Partington, 1935) and molecular iodine (I_2) with HNO_3. Note also that I_2O_4 reacts slowly to form HIO_3 in water though is not decomposed by moist air (Daehlie and Kjekshus, 1964b).

$$5\ I_2O_4 + 4\ H_2O \rightarrow I_2 + 8\ HIO_3$$

This reaction scheme evinces the impossibility of producing I_2O_4 particles with the nebuliser since I_2O_4 would be converted to HIO_3 in water and once heated in the thermo-denuder it would give I_2O_5. Upon heating I_2O_4 decomposes into I_2O_5 and iodine, which is lost by sublimation (Daehlie and Kjekshus, 1964a; Greenwood and Earnshaw, 1997)

$$5\ I_2O_4 \xrightarrow{135°–190°C} I_2 + 4\ I_2O_5$$

Therefore the reference systems studied in this work are HIO_3 and I_2O_5.

2.2.2 Photochemical reaction of CH_2I_2 with O_3

In order to investigate the volatile and hygroscopic properties of I_2O_4 a photochemical reactor chamber was designed (Fig. 2). Particles were generated by photolysis of CH_2I_2 in the presence of O_3 and UV-light. The laminar-flow stainless-steel reactor had a diameter of 11 cm and length of 102 cm, and was equipped with 12 inlets/outlets (4 along the external cylinder and 4 at each end of it) for the introduction of reactants and sampling of aerosol at different length of the cylinder (corresponding to different residence times). The fluorescence lamp (Philips TLD36W/08 with λ_{max}~365 nm ($300 < \lambda < 460$ nm)) was sealed in the cylinder and turned on during the experiment. The CH_2I_2 was evaporated over low heat, and the vapour carried into a Teflon/Tedlar bag using a known flow rate of nitrogen. Concentration of CH_2I_2 in the reactor was 20ppm. Ozone was produced by an ozone generator from dry air, scrubbed by passing it through charcoal. Its concentration was tested using ozone strips, and then diluted with dry filtered air so that its concentration was 230ppb. These concentrations were chosen to maximise the particle count ($>10^6 cm^{-3}$ required for analysis of monodisperse fractions of the distribution). The total flow rate through the reactor was 3 lpm. This corresponded to a total residence time of around 3 minutes. When larger particles were desired, an additional chamber of larger volume was employed to allow the particles more time to grow before entering the VH-TDMA system.

2.3 Raman Spectroscopy

The Raman spectra were acquired using a Renishaw Model 1000 microprobe spectrometer. The system includes an Olympus microscope to visualise the sample and to direct the exciting light onto the sample and collect the scattered light, an optical filter to remove the Rayleigh scattering line, in addition to a single diffraction grating and a change-couples device as the detector. The microscope is equipped with three interchangeable objective lenses with magnification 50, 20 and 10 respectively. Typically the 50 times objective was used. Raman spectra were excited with radiation at 633 nm from a Spectra-Physics Model 127 He-Ne laser with a maximum power of 10mW. The spectra were recorded with a resolution of $4cm^{-1}$ in the spectral region 4000-200 cm^{-1} and acquisitions were repeated to improve the signal-to-noise ratio.

2.4 Scanning Electron Microscopy (SEM)

Photooxidation product was collected for SEM analysis by drawing aerosol from the reaction chamber through a 0.5 mm diameter orifice at sonic speeds onto an impaction plate which consisted of a piece of cleaned silicon wafer. The resulting sample was stored in dry nitrogen in a sealed container prior to coating, for SEM analysis, with a thin conductive layer of carbon using a Cressington high vacuum evaporative coater.

The treated sample, and a similarly treated standard consisting of commercial I_2O_5, were analysed at 10kV accelerating voltage by energy-dispersive X-ray spectrometry (EDX) on an FEI Quanta 200 SEM fitted with an EDAX thin-window X-ray detector and microanalysis system.

2.5 Chemicals

The chemicals used included diiodopentoxide, I_2O_5 (Aldrich, 99.99% purity, d = 5.08 g/cm^3), diiodomethane, CH_2I_2 (Laboratory Unilab, d=3.3g/cm^3), NaCl (Merck AnalaR 99.9%) and ultra pure deionised water (Elga: Elgastat, 0.2 μS/cm at 25ºC).

3 RESULTS AND DISCUSSION

3.1 Nebulisation of a water solution (HIO_3/I_2O_5 aerosols)

Volatility/hygroscopicity analyses were carried out on 27 nm, 75 nm (shown on Fig. 3) and 102 nm HIO_3 particles in nitrogen as a sheath and carrier gas. The particles' mobility diameters after volatilization and after subsequent humidification were measured as the temperature was stepped up to a maximum of 350°C, in increments of 5-20°C, with the smaller increments employed over periods of rapid shrinkage.

The temperature behaviour in N_2 shows rapid reduction in mobility diameter beginning at 210°C (region I), a slight plateau between 240 and 270°C (region II), followed again by swift shrinkage (region III) until only a non-volatile residue remains. The residue particles comprise <1% of the initial particle volume, and occur at such low concentration that the hygroscopic peaks cannot be distinguished from background noise, precluding determination of the nature of the residue particles by their growth factor. For larger initial mobility diameters, the temperature at which only residue remains is higher, following an apparently linear trend given by $T_c\,[°C] = 260 + 1.05 \times D_v\,[nm]$.

The volatility behaviour was similar in both filtered air (see full line in figure 4) and N_2, although in air the volatilization steps occur at lower temperatures, with rapid reduction in mobility diameter beginning at 190°C, a slight plateau at 205-230°C, and volatilisation complete by 290°C.

The onset of rapid shrinkage is accompanied by the appearance of a shoulder on the higher-diameter side of the peak in the hygroscopicity scans, which splits off to form a second peak of higher growth (the 'hygroscopic peak'); there is also an increase in the growth of the original peak (the 'non-hygroscopic peak') of approximately 10%.

These volatility characteristics in region I have been associated with the dehydration of HIO_3 via the intermediate product $HIO_3 \cdot I_2O_5$, and, as the temperature increases, to I_2O_5. The observed hygroscopic growth seems to correlate with the formation of I_2O_5 at 210°C. As the hygroscopic growth is correlated to I_2O_5, the more HIO_3 is converted to I_2O_5 the more hygroscopic material there is available and the hygroscopic growth factor (G_h) increases. In region II all of the HIO_3 is converted into I_2O_5 and G_h remains constant. The temperature is still not sufficiently high to induce rapid evaporation of I_2O_5 and we observe a slight plateau

in the volatility curve. Above 270°C, in region III, I_2O_5 starts to evaporate rapidly until it totally evaporates at 336°C.

On the other hand since the differences in density are such that a HIO_3 particle would be 5% greater in diameter than a I_2O_5 particle containing equivalent iodine, the rise in non-hygroscopic growth near 210°C may be partly due to re-hydration of I_2O_5 back to HIO_3 in the humidifying column.

Hygroscopic growth data for HIO_3 particles was collected in the RH range of 80-98%, using N_2 as the sheath gas. Despite its high solubility, HIO_3 was found not to be hygroscopic at room temperature; no significant growth was displayed until the thermodenuder temperature reached 200°C or above. At 223°C, 88 nm particles exhibit hygroscopic growth at humidities above 89%**.**

The measured growth factors were low for an ionic solid. This is consistent with previous observations of associated species such as $(HIO_3)_2$, $(HIO_3)_3$ and $[H(IO_3)_2]^-$ in concentrated HIO_3 solutions (Greenwood and Earnshaw, 1997; Paitnik, 2003), which would result in a higher vapour pressure than would be found above a dissociated salt solution. Double peaks were generally observed in the hygroscopicity scans, with one peak showing little or no growth (G = 0.95-1.1), and a second peak exhibiting humidity-dependent growth (G = 1.3-2). These will be referred to as the non-hygroscopic and hygroscopic peaks respectively, with growth factors G_{nh} and G_h. Hygroscopic growth is only observed at high temperature (T~ 200 °C or above) While only a limited number of growth measurements were taken with filtered air as the sheath instead of N_2, the results indicate that the hygroscopic growth factor is independent of sheath composition.

3.2 Photochemical reaction of CH_2I_2 with O_3

The volatility characteristics as well as the temperature dependent hygroscopic growth were also determined for particles generated in the nucleation chamber via photolysis of CH_2I_2 in the presence of O_3, and are presented on Figure 4. Previous studies (Burkholder et al., 2003; Cox and Coker, 1983; Hoffmann et al., 2001; Jimenez et al., 2003) suggest that such particles may be composed of I_2O_4, formed as a polymer of OIO units which are initiated by the reaction of ozone with iodine radicals:

$$CH_2I_2 + h\nu \rightarrow I + CH_2I$$

$$I + O_3 \rightarrow IO + O_2$$

$$IO + IO \rightarrow OIO + I$$

$$OIO + OIO \rightarrow I_2O_4 \quad (\text{or } [IO]^+[IO_3]^-)$$

$$I_2O_4 + nOIO \rightarrow\rightarrow [\text{-I-O-}IO_2\text{-O-}]_{1+n/2}$$

Particles exiting the photochemical reactor were collected over a period of several hours (2-3 hr).

The volatility behaviour of these nucleated particles is similar to that of HIO_3 particles in a filtered-air sheath (see full line in Fig. 4). Three regions in the volatility curve can also be observed, but the width of these regions is much narrower than in the previous case. I_2O_4 particles first reduction in size appears at 190°C (region I) to be followed by a small plateau from 205-220°C (region II), and with a rapid shrinkage (region III) up to temperatures of 290°C where all of the particle evaporates.

Similarly to the previous case, with HIO_3/I_2O_5 particles, hygroscopic peaks were only observed at high temperatures and humidities, and double peaks were present, a hygroscopic (G_h) and a nonhygroscopic (G_{nh}) one. Particle shrinkage at 190°C was accompanied by an increase in G_{nh} of approximately 10 %. While this may suggest that the particles are either formed as HIO_3 or convert to it within the chamber, this is not necessarily the case, as I_2O_4 also transforms into I_2O_5 at temperatures above 190°C (Daehlie and Kjekshus, 1964a).

While the hygroscopic peak in the HIO_3/I_2O_5 system appeared since the onset of shrinkage in region I, in this system the hygroscopic peak only appeared in region II for temperatures above 205°C. The growth factors were again low, generally agreeing with the HIO_3/I_2O_5 growth model predictions (see appendix) to within 3%

3.3 Raman analysis

The particles were collected and placed between quartz plates for the spectra acquisition. Figures 5 and 6 shows the Raman spectra of HIO_3, I_2O_5, the photochemically produced aerosols (labelled I_2O_4) and I_2O_5 powder (from Aldrich) in the range 850-200cm^{-1} and 3750-1500 cm^{-1}, respectively. The relative intensities of the I_2O_5 and I_2O_4 spectra in Fig. 6 have been multiplied by a factor 10. Comparison with reference spectra of HIO_3, I_2O_4 and I_2O_5 from the literature was done with the intent of identifying the different types of oxides and

oxyacids. (Dalziel et al., 1976; Dasent and Waddington, 1960; Dasent and Waddington, 1963; Ellestad et al., 1981; Sherwood and Turner, 1970; Sunder and Vikis, 1987; Sunder et al., 1985) However, the comparison is not straightforward, since the aerosols were formed and exposed to ambient condition (RH ~ 30-50 %) while many references spectra were taken under vacuum. In addition the nucleating particles are in the range of nanometers while the references were compounds in liquid phase or large crystals. Furthermore the literature data are not always in agreement in the assignment of spectral bands.

All the spectra presented in Fig. 5 are characterized by intense bands between 800-700cm^{-1} assigned to symmetric and anti-symmetric I=O and IO_2 stretching modes. The spectrum of I_2O_5 powder (Aldrich) is shown in Fig. 5 (dark plot); the compound, once exposed to ambient air is rapidly converted to its partially hydrate form $I_2O_5 \cdot HIO_3$ also defined as HI_3O_8. This is confirmed by the bands at 810, 745, 642, 452 and 236cm^{-1} assigned to HI_3O_8 (Durig et al., 1965; Sherwood and Turner, 1970). The spectrum shows a fine structure that gives indication of a certain degree of crystallinity, while the aerosols produced by atomisation of the water solution do not show fine structure at low frequencies (Fig. 5). This could to be correlated to the water content (see also Fig. 6) which is abundant in the later case, despite the fact that all samples have been exposed to similar ambient condition and size of the particles (low degree of order for small particles). In addition, particles in the nanometer size range may absorb water more easily than larger particles, due to their high surface area.

HIO_3, red plot, has very broad bands, which may indicate an amorphous or pseudo-liquid state. Comparison with the literature (Durig et al., 1965; Sherwood and Turner, 1970) shows that HIO_3 particles have mixed features characteristic of a high concentrated solution of HIO_3 (bands at 823, 776, 757, 739 cm^{-1}) and a crystalline form (bands at 765, 728 cm^{-1}). Bands at 776 and 757 cm^{-1} have also been observed in $NaNO_3$ spectra and are associated to the presence of dissociated iodate ions (Dasent and Waddington, 1960; Durig et al., 1965). Figure 6 suggests that these ions might be present because of the large amount of free water with broad bands at 3350, 3100 cm^{-1} assigned to anti-symmetric and symmetric stretching and a band at 1660cm^{-1} due to bending mode. The less intense peak at ~ 2900cm^{-1} has been assigned to H-O stretching of undissociated H-O in HIO_3. (Dasent and Waddington, 1960; Durig et al., 1965)

I_2O_5 particles, green plot in Fig. 5, show minor broadening with respect to HIO_3 particles. This could be explained in term of less water absorbed and a more organized structure. The H-O stretching of undissociated HIO_3 is present at ~ 2900 cm^{-1}, water bands at ~ 3100 and 3025 cm^{-1} are present. Bands at 739 and 728 cm^{-1} are associated with crystalline HIO_3. I_2O_5 particles formed upon heating HIO_3 in the thermodenuder at ca. 200C mainly exhibit features of crystalline HIO_3.

Particles formed upon photo-oxidation of diiodomethane in the presence of ozone have also been collected and analysed, blue plot (Figs. 5 and 6). The spectrum surprisingly presents bands at 756, 739 and 728 cm^{-1} typical of crystalline HIO_3. However the stretching mode of HIO_3 is not visible and little water seems to be present. The typical stretching modes of free water are relatively weak and the bending mode at 1660cm^{-1} is absent (Fig. 6). The intense stretching bands that should identify crystalline I_2O_4 or I_2O_5 were not present.

3.4 SEM ANALYSIS

Figure 7. shows the I_2O_5 standard and photooxidation product comparison EDX spectra. The standard was used to calibrate the system for relative X-ray intensities of iodine and oxygen. The photooxidized sample was found to contain iodine/oxygen in the mass ratio 4.03 with a 10% error, which compares well with the expected value of 3.97 for I_2O_4. Besides X-ray peaks for oxygen and iodine, only peaks from the carbon coating and the silicon substrate were present in the X-ray spectra, indicating that no other elements were present at levels above about 0.2 weight%.

4 Conclusions

Iodine aerosol particles were produced in two different ways by nebulising a water solution of I_2O_5 and by photochemical reaction of CH_2I_2 with O_3. As I_2O_5 reacts with water producing HIO_3 the first method resulted in the production of HIO_3 aerosol particles at room temperature. To produce I_2O_5 particles, HIO_3 aerosols were heated in a thermodenuder to temperatures above 200°C. The photochemical reaction of CH_2I_2 with O_3 resulted in production of I_2O_4 particles. This was confirmed by EDX spectroscopy that showed that the mass ratio iodine to oxygen was 4.03 which compares well with the expected value of 3.97.

The temperature dependence of the diameter of HIO_3 particles in N_2 as sheath gas shows rapid reduction in size beginning at 210°C, a slight plateau between 240 and 270°C, followed again by swift shrinkage up to 340°C until only a non-volatile residue remains. The volatility behaviour was similar in both filtered air, although in air the volatilization steps occur at lower temperatures, with rapid reduction in size beginning at 190°C, a slight plateau at 205-230°C, and volatilisation complete by 290°C. The volatility of particles generated in the chamber by photolysis of CH_2I_2 in the presence of O_3 was very similar to that of HIO_3 aerosols when air was used instead of N_2 as the sheath gas.

All of the analysed aerosols showed hygroscopic growth only after they were heated to temperatures above 200°C. This would lead to the conclusion that neither HIO_3, which is a very soluble substance, nor I_2O_4 exhibit any hygroscopic growth, as both HIO_3 and I_2O_4 transform into I_2O_5 at 200°C and 190°C respectively.

The Raman spectra indicate that once the particles are exposed to ambient conditions, they tend to absorb more or less water and independently of their original structure tend to be converted with time into HIO_3. I_2O_5 particles were able to adsorb water in a much more efficient way than the particles formed upon photo-oxidation of diiodiomethane. The spectra do not allow a determination of their original form, but they give an indication of a different aerosols "predisposition" to absorb water and of the lack of impurities. Raman analysis of particles was performed under ambient condition because formation and collection of the sample was impossible under vacuum conditions, but even under controlled conditions the differences in the stretching modes between HIO_3, I_2O_4 and I_2O_5 are so marginal that a secure identification of the aerosol is not possible with this technique.

Appendix A: Mathematical background

Growth model

A model to describe the growth of HIO_3/ I_2O_5 was created based on a general model for ionic salts described by Wei Li (1992), with a correction in the form of the osmotic coefficient to account for deviation from Raoult's law.

The water activity and osmotic coefficient φ of a solution are defined as

$$a_w = \frac{p_{f,sol}}{p_{f,w}}$$
$$\varphi = \frac{-\ln a_w}{mvM_w} \quad (1)$$

The Kelvin equation is used to take into account the curved surface of a spherical droplet:

$$\frac{p_{c,sol}}{p_{f,sol}} = \exp\left(\frac{4\sigma M_w}{RT\rho d}\right) \quad (2)$$

The particle is in equilibrium with its surroundings when

$$H = \frac{p_{c,sol}}{p_{f,w}} \quad (3)$$

A good approximation can be made of the density by assuming additivity of the masses and volumes of the components:

$$\rho = \frac{m_w + m_s}{V_w + V_s} \quad (4)$$

Finally, an analytical function representing φ was created based on reported freezing point depressions and boiling point elevations of HIO_3 solutions (Mellor, 1922; Washburn et al., 2003) adjusted to 25°C:

$$\varphi = 2.694 - 0.8627\sqrt{\mathrm{m}} + 0.08282\mathrm{m} - 0.00008297\mathrm{m}^{3/2} - 1.541e^{-0.1\mathrm{m}} - 0.1518e^{-2.7\mathrm{m}} \quad (5)$$

Note that since I_2O_5 reverts to HIO_3 in solution, this expression is relevant for predicting the growth of both I_2O_5 and HIO_3 particles. When the above information is combined, the resulting model predicts relatively low growth factors, and yields a deliquescence humidity of 85% for arbitrarily large particles. Figure 8 shows a comparison between the theoretical model and the measured growth factors of 90nm HIO_3 particles that were heated to a temperature of 220°C. The deliquescence humidity was observed to lie between 85.5% and 89%, which compares quite well with the predicted value of 85.5% for 90nm particles

It must be noted that the experimentally measured growths do not necessarily represent the growth of HIO_3, since the particles which grow are partly or wholly composed of I_2O_5. Thus the measured growths are expected to be up to 5% larger than those predicted by the HIO_3 model, depending on the extent of conversion of HIO_3 to I_2O_5 in the particle.

$p_{f,sol}$ equilibrium water vapour pressure above a solution with a flat surface

$p_{f,w}$ equilibrium vapour pressure above pure water (flat surface)

$p_{c,sol}$ equilibrium vapour pressure over the curved surface of the droplet solution

m molality

v number of ions per molecule of solute

a_w water activity

φ osmotic coefficient

M_w molecular weight of water in mol/kg

σ surface tension of water

ρ droplet density

d droplet diameter

H relative humidity

m_s, V_s mass and volume of the salt in the droplet

m_w, V_w mass and volume of water in the droplet

References

Ansari, A.S. and Pandis, S.N.: Water Absorption by Secondary Organic Aerosol and Its Effect on Inorganic Aerosol Behavior, Environmental Science and Technology, 34(1): 71-77, 2000.

Bahl, R.K. and Partington, J.R.: Lower oxides and sulfates of iodine, Journal of the Chemical Society, Abstracts: 1258-63, 1935.

Burkholder, J.B., Curtius, J., Ravishankara, A.R. and Lovejoy, E.R.: Laboratory Studies of the Homogeneous Nucleation of Iodine Oxides, Atmospheric Chemistry and Physics, 3: 4943-4988, 2003.

Chase, M.W.: NIST-JANAF thermochemical tables for the iodine oxides, Journal of Physical and Chemical Reference Data, 25(5): 1297-1340, 1996.

Cox, R.A. and Coker, G.B.: Absorption cross-section and kinetics of IO in the photolysis of CH 3 I in the presence of ozone, J. Phys. Chem, 87: 4478-4484, 1983.

Daehlie, G. and Kjekshus, A.: Iodine oxides, Part I, Acta Chem. Scand., 18: 144-156, 1964a.

Daehlie, G. and Kjekshus, A.: Iodine oxides. I. I2O3.SO3, I2O3.4SO3.H2O, I2O3.SeO3, and I2O4, Acta Chemica Scandinavica, 18(1): 144-56, 1964b.

Dalziel, J.R., Carter, H.A. and Aubke, F.: Iodine-oxygen compounds. 2. Iodosyl and iodyl fluorosulfates and trifluoromethane sulfates, Inorganic Chemistry, 15(6): 1247-51, 1976.

Dasent, W.E. and Waddington, T.C.: Iodine-oxygen compounds. II. Iodosyl and related compounds, Journal of the Chemical Society, Abstracts: 3350-6, 1960.

Dasent, W.E. and Waddington, T.C.: The infrared spectrum and structure of I2O4, Journal of Inorganic and Nuclear Chemistry, 25: 132-3, 1963.

Durig, J.R., Bonner, O.D. and Breazeale, W.H.: J. Phys.Chem., 69: 3886-3892, 1965.

Ellestad, O.H., Woldbaek, T., Kjekshus, A., Klaeboe, P. and Selte, K.: Infrared and Raman studies of crystalline iodine oxides (I2O5 and I2O4), iodosyl sulfate and iodosyl selenate, Acta Chemica Scandinavica, Series A: Physical and Inorganic Chemistry, A35(3): 155-64, 1981.

Greenwood, N.N. and Earnshaw, A.: Chemistry of the Elements (2nd Edition). Butterworth-Heinemann, 1341 pp, 1997.

Hoffmann, T., O'Dowd, C.D. and Seinfeld, J.H.: Iodine oxide homogeneous nucleation: An explanation for coastal new particle production, Geophysical Research Letters, 28(10): 1949-1952, 2001.

IPCC, 2001. Climate Change 2001: The Scientific Basis. Contribution of Working Group I to the Third Assessment Report of the Intergovernmental Panel on Climate Change, Cambridge University Press, Cambridge, United Kingdom and New York, NY, USA.

Jimenez, J.L., Bahreini, R., Cocker, D.R. et al.: New particle formation from photooxidation of diiodomethane (CH2I2), Journal of Geophysical Research-Atmospheres, 108(D10): -, 2003.

Johnson, G., Ristovski, Z.D., D'Anna, B. and Morawska, L.: The hygroscopic behavior of partially volatilized coastal marine aerosols using the VH-TDMA technique, Journal of Geophysical Research, 110(D20203): doi:10.1029/2004JD005657, 2005.

Johnson, G., Ristovski, Z.D. and Morawska, L.: Application of the VH-TDMA technique to coastal ambient aerosols, Geophysical Research Letters, 31: L16105, 2004a.

Johnson, G., Ristovski, Z.D. and Morawska, L.: Method for measuring the hygroscopic behavior of lower volatility fractions in an internally mixed aerosol, Journal of Aerosol Science, 35(4): 443-455, 2004b.

Kulmala, M., Korhonen, P., Napari, I. et al.: Aerosol formation during PARFORCE: Ternary nucleation of H2SO4, NH3, and H2O, Journal of Geophysical Research-Atmospheres, 107(D19): -, 2002.

Kulmala, M., Pirjola, U. and Makela, J.M.: Stable sulphate clusters as a source of new atmospheric particles, Nature, 404(6773): 66-69, 2000.

McFiggans, G.M., Coe, H., Burgess, R. et al.: Direct Evidence for Coastal Iodine Particles from Laminaria Macroalgea - Linkage to Emissions of Molecular Iodine, Atmospheric Chemistry and Physics, 4: 701-713, 2004.

Mellor, J.: A comprehensive treatise on inorganic and theoretical chemistry,, 2. Longmans, Green and Co., London, 1922.

Napari, I., Kulmala, M. and Vehkamaki, H.: Ternary nucleation of inorganic acids, ammonia, and water, Journal of Chemical Physics, 117(18): 8418-8425, 2002.

O'Dowd, C.D., Geever, M., Hill, M.K., Smith, M.H. and Jennings, S.G.: New particle formation: nucleation rates and spatial scales in the clean marine coastal environment, Geophysical Research Letters, 25(10): 1661-1664, 1998.

O'Dowd, C.D., Hameri, K., Makela, J. et al.: Coastal new particle formation: Environmental conditions and aerosol physicochemical characteristics during nucleation bursts, Journal of Geophysical Research-Atmospheres, 107(D19): art. no.-8107, 2002a.

O'Dowd, C.D., Hameri, K., Makela, J.M. et al.: A dedicated study of New Particle Formation and Fate in the Coastal Environment (PARFORCE): Overview of objectives and achievements, Journal of Geophysical Research-Atmospheres, 107(D19): art. no.-8108, 2002b.

O'Dowd, C.D., Jimenez, J.L., Bahreini, R. et al.: Marine aerosol formation from biogenic iodine emissions., Nature. Nature Publishing Group, pp. 632, 2002c.

Paitnik, P.: Handbook of inorganic chemicals. McGraw-Hill, New York, 2003.

Rader, D.J. and McMurry, P.H.: Application of the Tandem Differential Mobility Analyzer to Studies of Droplet Growth and Evaporation, J. Aerosol Sci., 17: 771-788, 1986.

Saiz-Lopez, A. and Plane, J.M.C.: Novel Iodine Chemistry in the Marine Boundary Layer, Geophysical Research Letters, 31: L04112, 2004.

Sherwood, P.M.A. and Turner, J.J.: Vibrational spectra of compounds in the iodine pentoxide-water system and sodium iodate, Spectrochimica Acta, Part A: Molecular and Biomolecular Spectroscopy, 26(10): 1975-92, 1970.

Sunder, S. and Vikis, A.C.: Raman spectra of iodine oxyacids produced by the gas-phase reaction of iodine with ozone in the presence of water vapor, Canadian Journal of Spectroscopy, 32(2): 45-8, 1987.

Sunder, S., Wren, J.C. and Vikis, A.C.: Raman spectra of iodine oxide (I4O9) formed by the reaction of iodine with ozone, Journal of Raman Spectroscopy, 16(6): 424-6, 1985.

Twomey, S.A., Piepgrass, M. and Wolfe, T.L.: An assessment of the impact of pollution of global cloud albedo, Tellus, Series B: Chemical and Physical Meteorology, 36B(5): 356-66, 1984.

Vakeva, M., Kulmala, M., Stratmann, F. and Hameri, K.: Field measurements of hygroscopic properties and state of mixing of nucleation mode particles, Atmospheric Chemistry and Physics [online computer file], 2: 55-66, 2002.

Van Dingenen, R. and Raes, F.: Ternary nucleation of methane sulfonic acid, sulfuric acid and water vapor, Journal of Aerosol Science, 24(1): 1-17, 1993.

Washburn, E.W., West, C.J. and Dorsey, N.E.: International critical tables of numerical data, physics, chemistry, and technology. Norwich, NY: Knovel, 2003.

Wei Li, Montassier, N. and Hopke, P.: A system to measure the hygroscopicity of aerosol particles, Aerosol science and Technology, 17: 25-35, 1992.

Wyslouzil, B.E., Seinfeld, J.H., Flagan, R.C. and Okuyama, K.: Binary nucleation in acid-water systems. II. Sulfuric acid-water and a comparison with methanesulfonic acid-water, Journal of Chemical Physics, 94(10): 6842-50, 1991.

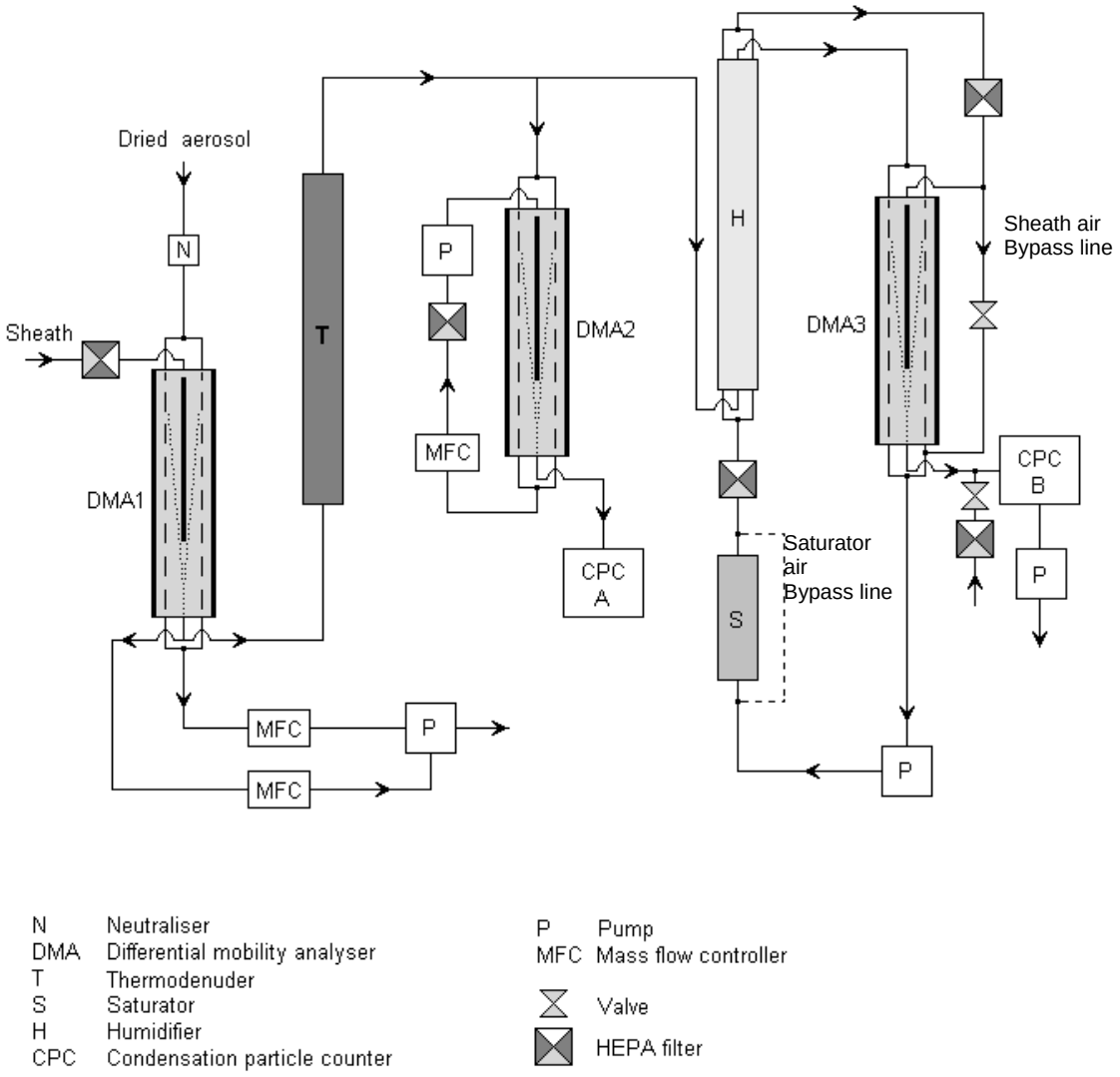

Figure 1. Schematic diagram of the VH-TDMA system.

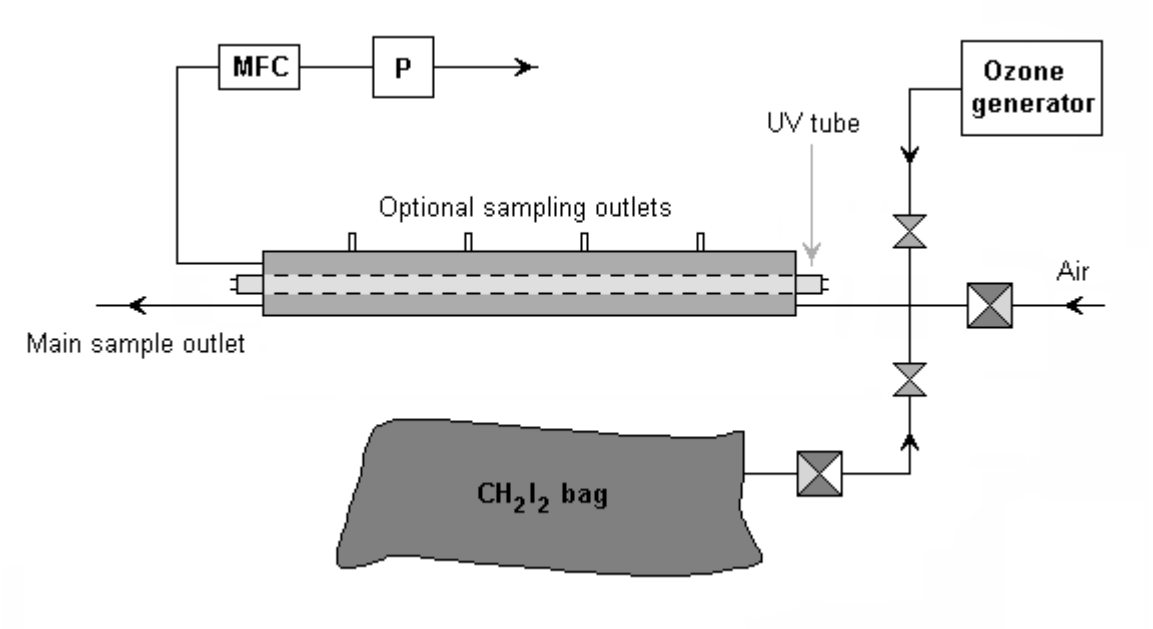

Figure 2. Photochemical reactor set-up. The chamber has optional outlets along the side to allow determination of the progress in aerosol growth. MFC – mass flow controller; P – pump.

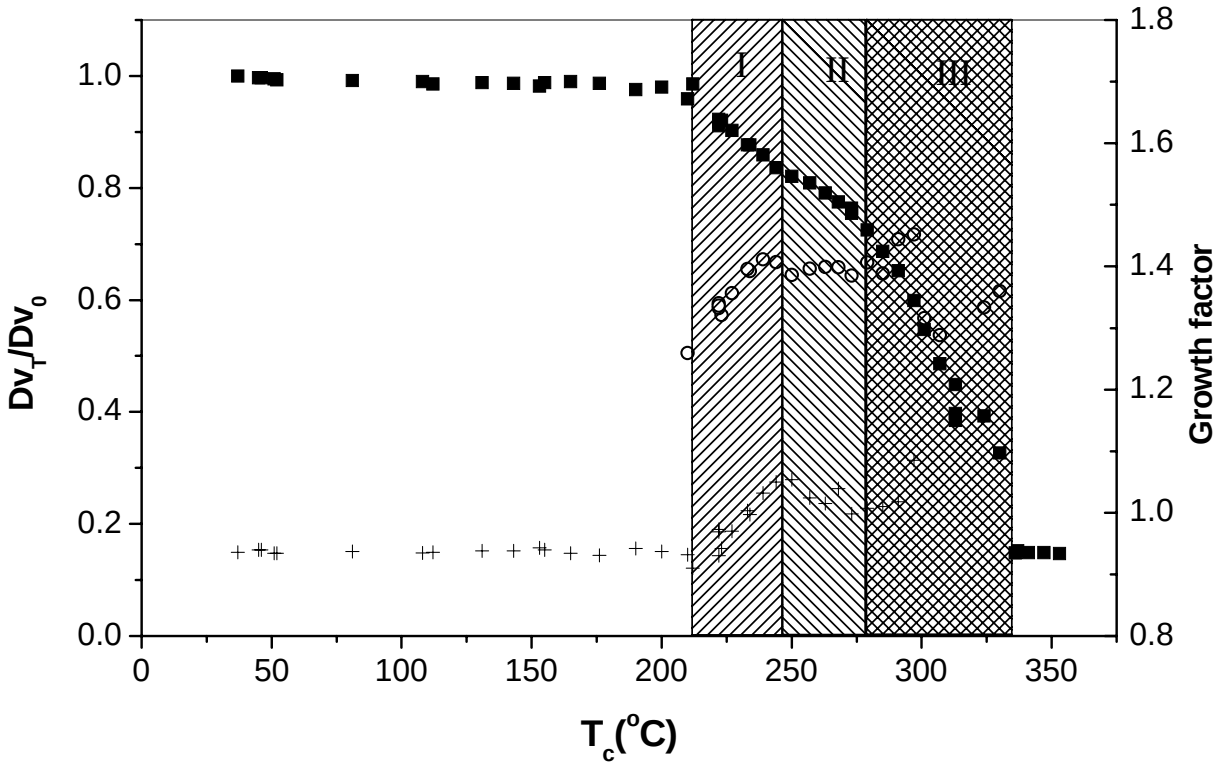

Figure 3. VH-TDMA spectra of HIO_3 particles with an initial diameter of 75nm, showing the relative diameter after volatilisation Dv_T/Dv_o – full squares; and the hygroscopic growth factors $G=D_h/D_v$ versus thermodenuder temperature, for both hygroscopic G_h (circles) and non-hygroscopic G_{nh} (crosses) peaks. Nitrogen was used as the sheath gas.

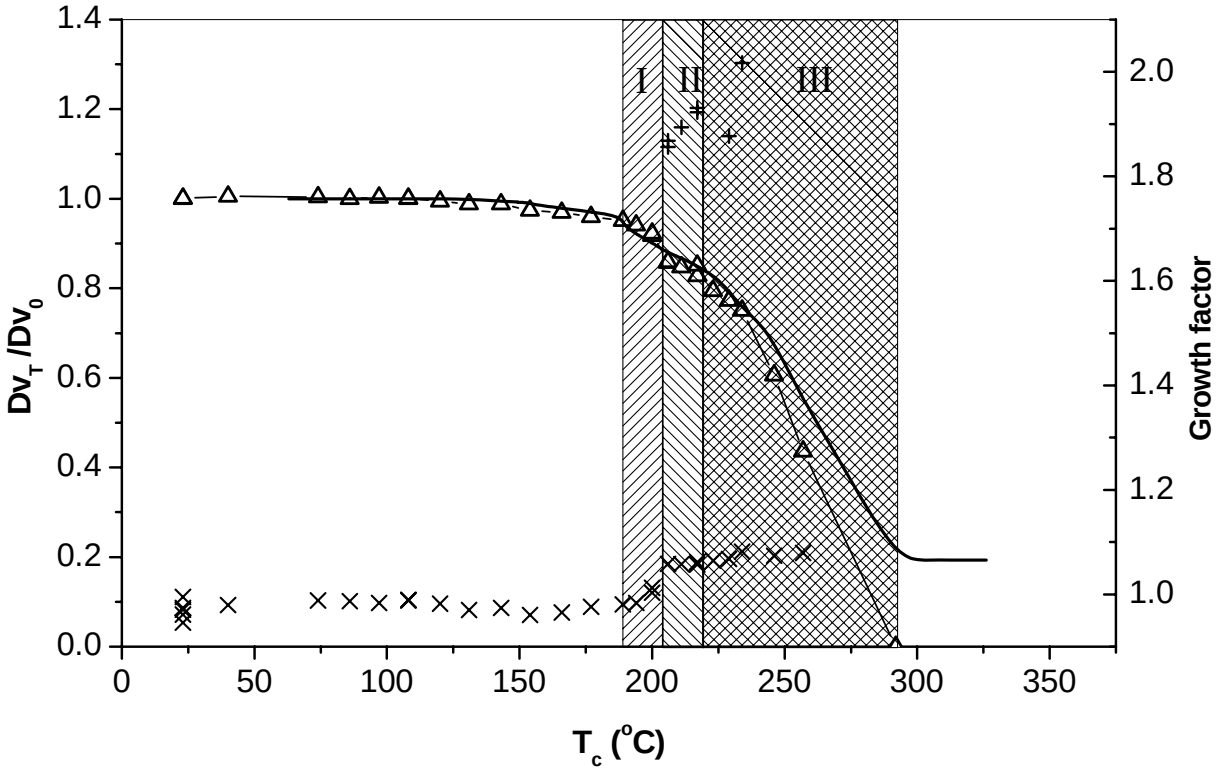

Figure 4. VH-TDMA spectra of 80 nm photochemically produced aerosols, showing the relative diameter after volatilisation Dv_T/Dv_o – triangles; and the hygroscopic growth factors $G=D_h/D_v$ versus thermodenuder temperature, for both hygroscopic G_h (+) and non-hygroscopic G_{nh}(×) peaks. The sheath gas was filtered air. The volatility curve of HIO_3 particles of similar size measured in air as sheath gas is also shown with a full line.

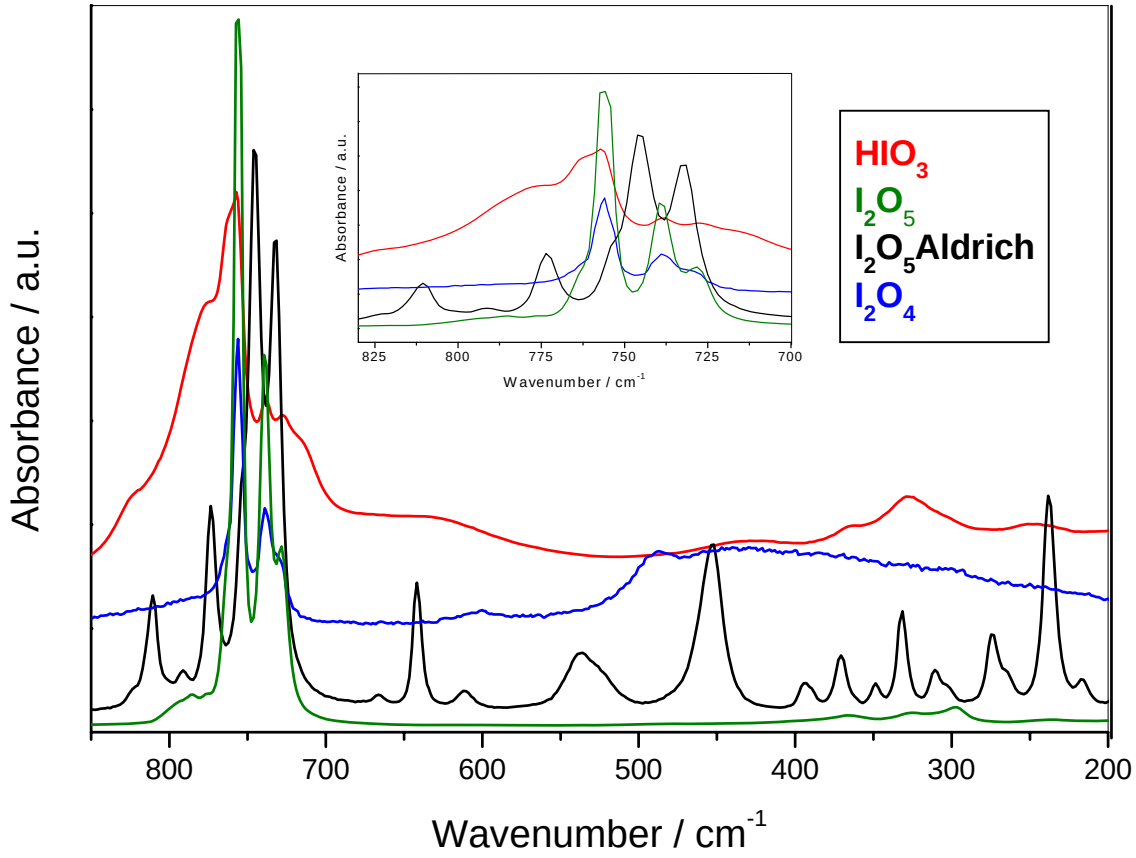

Figure 5. Raman spectra of HIO_3, I_2O_5 and the photochemically produced aerosols together with I_2O_5 powder (from Aldrich) in the range 1000-200cm^{-1}

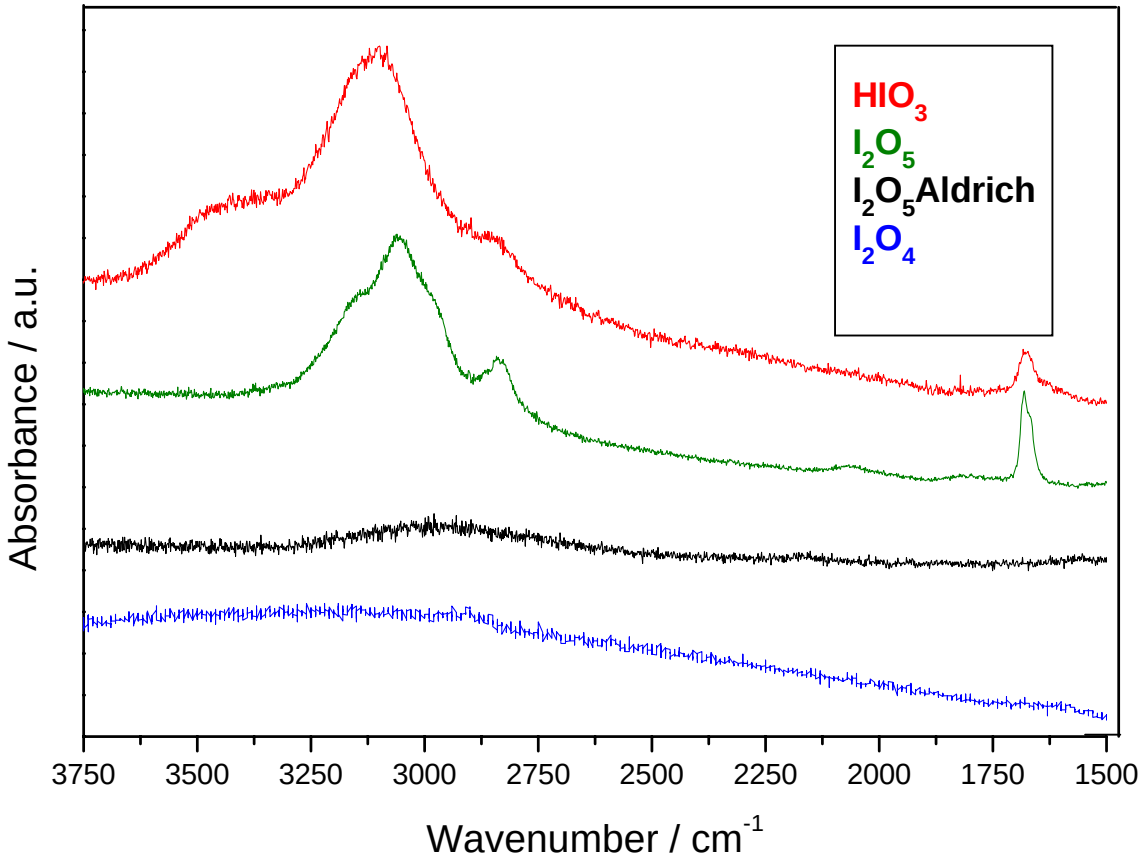

Figure 6**.** Raman spectra of HIO_3, I_2O_5 and the photochemically produced aerosols together with I_2O_5 powder (from Aldrich) in the range 4000-1000 cm^{-1}.

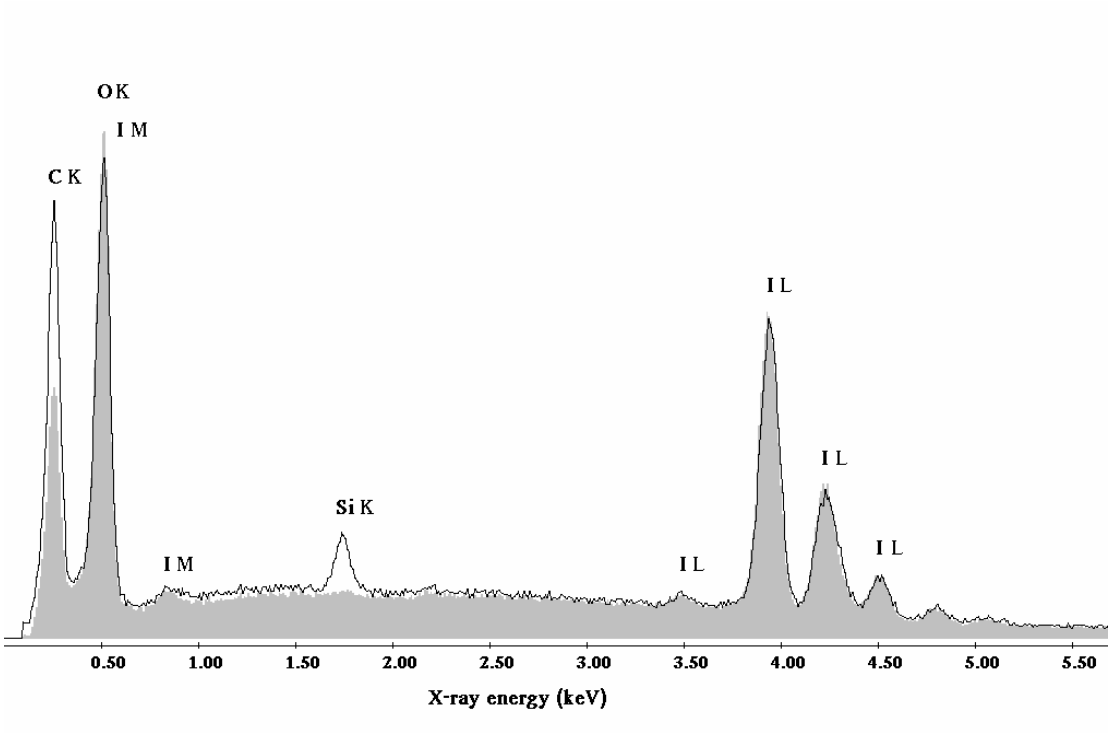

Figure 7: I_2O_5 (in light grey) and the photooxidation product (black line) comparison spectra.

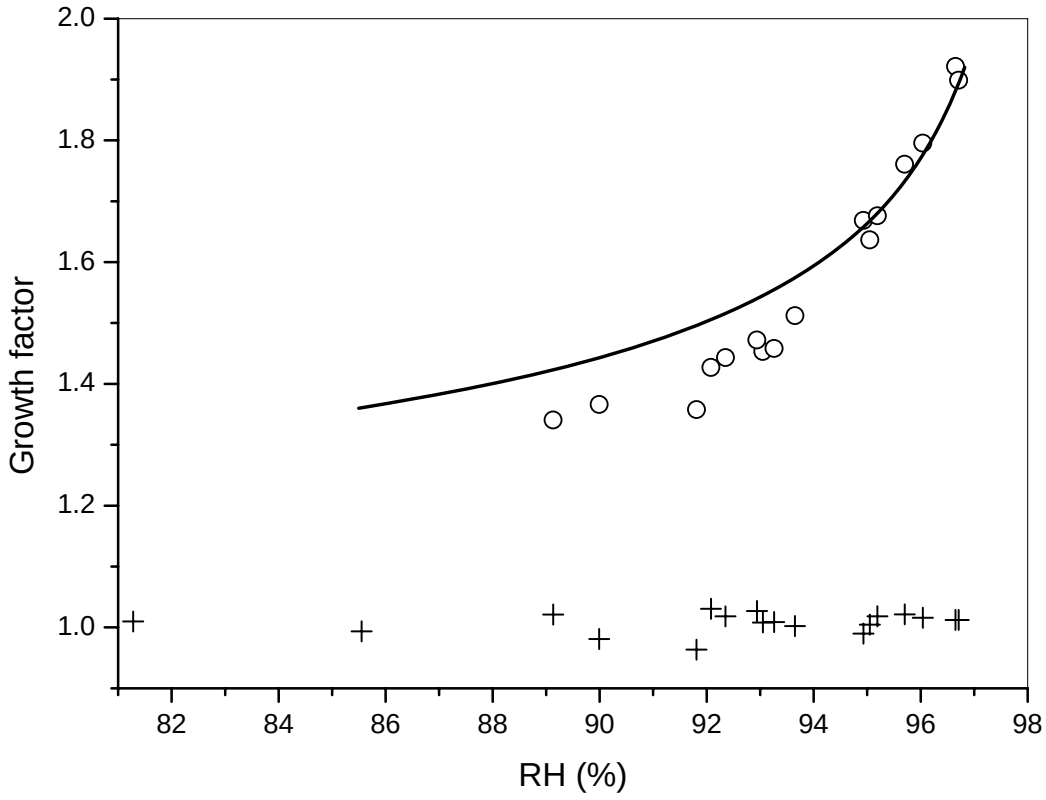

Figure 8 Hygroscopic growth factor versus relative humidity for 90nm HIO_3 particles heated to 220°C in a sheath of N_2: circles – hygroscopic growth factor, crosses – non-hygroscopic growth factor, full line – model predictions for HIO_3 particles.